Investigating apparent plateau phases in fatigue after impact damage growth in CFRP with ultrasound scan and acoustic emissions

Biagini, Davide; Pascoe, John Alan; Alderliesten, René

DOI
10.1016/j.ijfatigue.2023.107957

Publication date
2023

Document Version
Final published version

Published in
International Journal of Fatigue

International Journal of Fatigue 177 (2023) 107957

Contents lists available at ScienceDirect

International Journal of Fatigue

journal homepage: www.elsevier.com/locate/ijfatigue

Investigating apparent plateau phases in fatigue after impact damage growth in CFRP with ultrasound scan and acoustic emissions

Davide Biagini *, John-Alan Pascoe, René Alderliesten

Aerospace Structures & Materials Department, Faculty of Aerospace Engineering, Delft University of Technology, Kluyverweg 1, 2629 HS Delft, The Netherlands

ARTICLE INFO

Keywords:
Fatigue
Delamination
BVID
CAI
LVI

ABSTRACT

In previous literature, a plateau phase in fatigue growth of impact delamination projected area in CFRP was found. Explaining this plateau phase still represents a knowledge gap. In the present work, echo-pulse and through thickness transmission ultrasonic scan inspections were combined with acoustic emission monitoring to explain this plateau phase. Before the onset of growth outside of projected area, growth of delamination in the central impact cone and growth of smaller delamination was observed. Low-frequency acoustic emissions localized in the impact damage were recorded even before any type of growth was measured. The provided evidence suggests that an actual plateau phase may not exist if all the damage mechanisms are properly considered.

1. Introduction

Carbon Fiber Reinforced Polymer (CFRP) laminates outperform metal alloys in terms of in-plane specific strength, but are known to behave poorly if subjected to dynamic out of plane loading, such as impacts. Impact damage in CFRP typically forms internally and consists of intralaminar matrix cracking, interlaminar cracking (delamination) and fiber fracture [1,2]. This internal damage acts as a stress raiser and constitutes a preferential initiation site for fatigue [3]. Of all the load cycles, compressive load cycles are the most critical, causing unstable failure modes like fiber kinking [4] and delamination growth driven by sub-laminate buckling [5,6]. Due to the low detectability of impact damage and the risk of in-service fatigue propagation, compression after impact fatigue of CFRP has been researched with great attention over the past decades, in particular in the aerospace sector [7].

A common experimental practice followed by researchers consists of monitoring delamination using ultrasound inspection at different stages of a compression fatigue after impact (CFAI) test, to track and describe its growth throughout the fatigue life. Following this procedure, a number of CFAI tests reported a phase in which no fatigue growth happened outside of the projected impact delamination area [3,8,9]. After this phase, a single delamination started growing outside of the damage envelope. When this 'plateau' phase in the growth of projected delaminated area was observed, it occupied a major part of fatigue life. In other works, instead, a gradual growth of delamination outside the damage envelope was observed from the beginning of the fatigue life [10,11]. The presence of this phase of no observable growth of delamination occupying a central phase in fatigue life still represents a knowledge gap [7,12]. What happens during this 'plateau' phase, and what triggers the sudden growth of delamination in the final stages of fatigue life?

It is essential to investigate this issue since the damage-tolerant design of various applications, such as civil aircraft [13,14], depends on the identification of load thresholds for 'no-growth' of fatigue.

Regarding this issue, Pascoe [12] hypothesized that the 'no-growth' phase could be a misconception caused by limitations of the ultrasound inspection technique. We know that impact damage is composed by multiple delaminations situated in different interfaces. Due to the shadowing phenomenon, it is not possible to observe any delamination which is positioned in a central depth between larger delaminations [15]. It is then possible that, while no growth was observed for a large part of the fatigue life, damage was propagating undetected by the C-scan, in the form of growth of shadowed delaminations.

A second aspect neglected in previous experimental fatigue studies, regards delamination growth inside the 'non-delaminated impact cone'. It was observed that below the impact dent, impact damage presents an area with less or no delamination, caused by the out of plane compression introduced in the contact with the impactor. In their compression after impact (CAI) test campaign, Bull et al. [16] compared the computed tomography (CT) scans of impacted specimens with the CT

* Corresponding author.
E-mail address: D.Biagini-1@tudelft.nl (D. Biagini).

https://doi.org/10.1016/j.ijfatigue.2023.107957
Received 29 May 2023; Received in revised form 13 September 2023; Accepted 18 September 2023
Available online 19 September 2023

scans of impacted specimens loaded in compression to a near-failure load. The loaded specimens showed a growth of delamination below the impact cone, with little delamination growth outside of the external damage area. This observation was performed in a static test; however it is reasonable to assume that a similar phenomenon may occur in fatigue. Unfortunately, the same investigation was not replicated in fatigue, probably due to the difficulty in performing CT scans in loco during fatigue tests. Additionally, it is hard to observe this phenomenon using ultrasound scanning due to the reflection caused by the curved surface of the impact dent. It could be that, while no growth was observed in previous tests, actually some growth of delamination occurred inside the non-delaminated cone.

A third aspect to consider is that, although impact damage includes transverse matrix cracks and fiber damage, most of the previous research has primarily targeted the fatigue growth of delaminations. Ultrasound inspections are suitable for identifying free surfaces that are oriented perpendicular to the velocity of the ultrasonic waves. In all the aforementioned studies, inspections were carried out perpendicular to the surface of the laminate, with the primary objective of identifying delamination. It is possible that, while no growth was observed in the delaminated region, other types of damage, such as intra-laminar matrix cracking, may have been propagating.

In summary, the available evidence seems to indicate that an actual plateau phase may not exist. It is more likely that during the initial phase of the CFAI tests, damage accumulates not detected by the ultrasound inspections but still contributes to the strength degradation.

One potential approach that could be used to perform a detailed investigation of the fatigue damage propagation, is acoustic emission (AE) monitoring. AE monitoring is a passive, non-destructive structural health monitoring technique in which piezo-electric sensors are utilized to monitor surface oscillations in solid materials. Every time a damage event occurs, acoustic waves are generated inside the material and travels towards the surfaces where a sensor records them and convert them into signals. This methodology provides three main advantages [17]: real-time damage detection during testing, the ability to localize damage using multiple sensors, and the potential to distinguish between different damage modes based on the different signal features generated by different source mechanisms. Several attempts to separate damage modes have been presented in the literature, using clustering and supervised classification of signals based on specific features [18,19].

The biggest challenges when analysing AE data in CFRP, are dealing with attenuation and with reflections. Acoustic waves undergo attenuation as they travel through the composite material, leading to modifications in signal parameters such as peak amplitude reduction. There is evidence from a modelling study [20], that frequency features may be less affected by attenuation. Averaged frequency quantities in particular, such as the centroid frequency, averaged peak frequency and partial powers, appear to perform well in damage mode separation [20]. Acoustic waves are reflected by the highly constrained edges of the CAI fixture. As a consequence, there is a risk for these reflections to be classified as new damage events. This effect can be reduced by positioning multiple sensors and performing localization. Unfortunately, increasing the number of sensors requires to size up the CAI specimens.

Despite these limitations, in different occasions AE monitoring studies have been performed in static CAI tests [21], in two cases implementing damage mode separation with different strategies [22,23]. There is however a lack of studies presenting acoustic emission analysis in fatigue CAI tests. Fatigue acoustic emission data analysis brings the additional complication of studying large datasets characterized by a higher noise level. Addressing these limitations, would allow for AE signal monitoring throughout the fatigue test, also during the phases of fatigue life in which no apparent growth is observed performing ultrasound inspections.

The present work aimed to better understand the plateau phase. In particular, the goal was to establish whether there is no damage growth, or instead damage mechanisms are active that are not detectable using the techniques employed in previous studies. To test whether indeed the plateau phase is an artefact of incomplete non-destructive inspection, we combined two types of ultrasounds inspections (echo pulse scan and through-thickness attenuation scan) with acoustic emission monitoring. Compared to previous works applying AE monitoring in CAI standard test, acoustic waveforms were localized in order to reduce noise and reflection effects. The frequency content of the waveforms from the entire fatigue test was used to study the different damage modes. Combining all the different monitoring techniques we were able to show that the plateau phase is not an actual plateau, since different damage accumulation mechanisms are active.

2. Methodology

2.1. Materials and manufacturing

For the CAI fatigue tests, a Toray M30SC Deltapreg DT120-200-36 UD carbon fiber/epoxy prepreg was laid up in $[-45, 0, 45, 90]_{4,S}$ orientation. The curing process was conducted in an autoclave (Fig. 1.a) using the manufacturer's recommended procedure, with a maximum pressure of 6 bar and a curing temperature of 120 °C. The curing cycle in the autoclave was applied to a large plate (400 × 600 mm) which then was cut into smaller rectangles (Fig. 1.c) using a circular diamond blade (Fig. 1.b). The final specimens had nominal dimensions of 150 × 100 × 5.15 mm, as specified in the ASTM D7136 standard. Using this methodology, a total of six specimen were manufactured. The unidirectional laminate properties (provided by the manufacturer) along 0-degree direction are an elastic modulus of 145 GPa, unidirectional strengths of 3010 MPa (tensile) and 1020 MPa (compressive). The static fracture toughness in mode I, obtained with standard DCB tests is 608 J/m^2.

2.2. Low velocity impact test

Impact testing was carried out in accordance with ASTM D7136 using a drop-weight tower, as shown in Fig. 2a. The support fixture had a cut-out with dimensions of 125 ± 1 mm in the length direction and 75 ± 1 mm in the width direction. To ensure single impacts, the impact tower was equipped with a catcher activated by optical sensors. A hemispherical impactor with a diameter of 16 mm and a mass of 4.8 kg was utilized. Following ASTM D7136's recommendation of 6.7 J per mm of laminate thickness, a target impact energy of 34 J was employed for all impacts. This resulted in a dent depth of <0.3 mm.

2.3. Fatigue test

The static CAI strength was determined in a previous work [13], where three specimens were subjected to static CAI tests in accordance with ASTM D7137. As there is no standardized method for fatigue CAI testing, the same setup as that used for static CAI testing was employed in the fatigue tests. Different specimens were tested at various compression load levels to obtain short life fatigue and long-life fatigue tests. We kept a constant R ratio (R = 10) and, to prevent self-heating of the specimens, a constant frequency of 3 Hz. The tests were conducted using an MTS hydraulic testing machine equipped with a 100 kN load cell. During the tests we recorded the applied force and the crosshead displacement.

2.4. Ultrasound inspection

To assess the size of delaminations, two ultrasound systems were utilized. The first system was a bespoke water-tank immersion system operating in through-transmission attenuation mode. This system uses a 5 MHz ultrasound frequency, with a distance of 100 mm between emitter and receiver. Scanning speed was set at 100 mm/s, resulting in a resolution of 1 mm. The second system adopted was the echo pulse

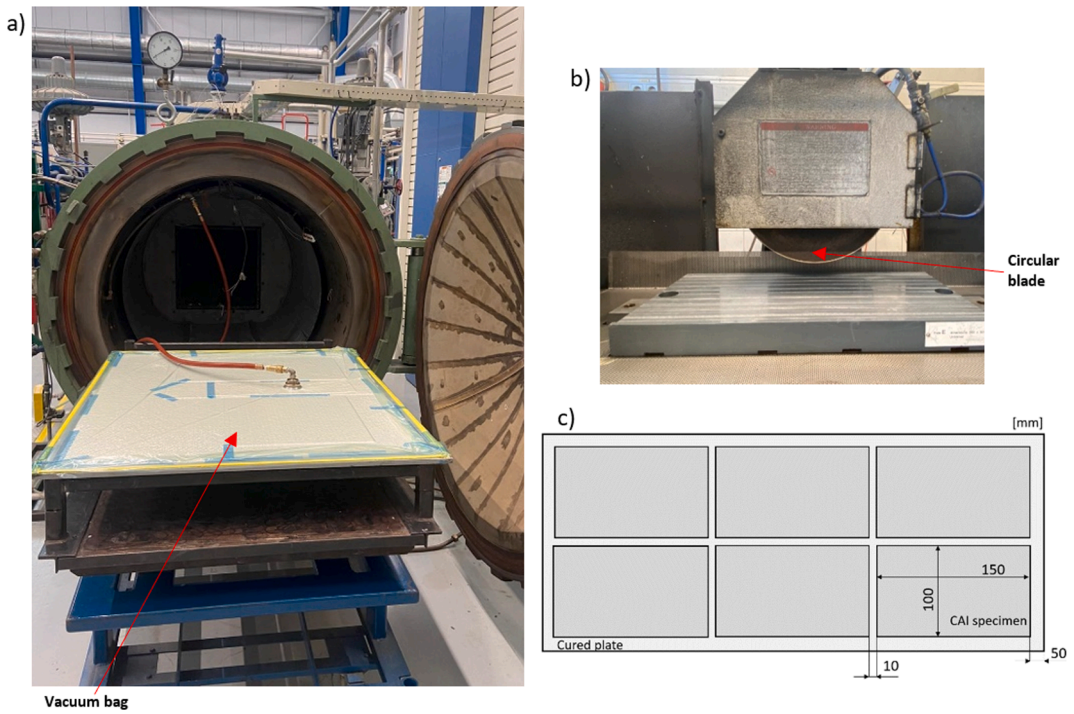

Fig. 1. (a) Autoclave used for curing CFRP plates; (b) Circular diamond blade cutter used to cut the specimens; (c) Cutting scheme to obtain CAI specimen from cured plates.

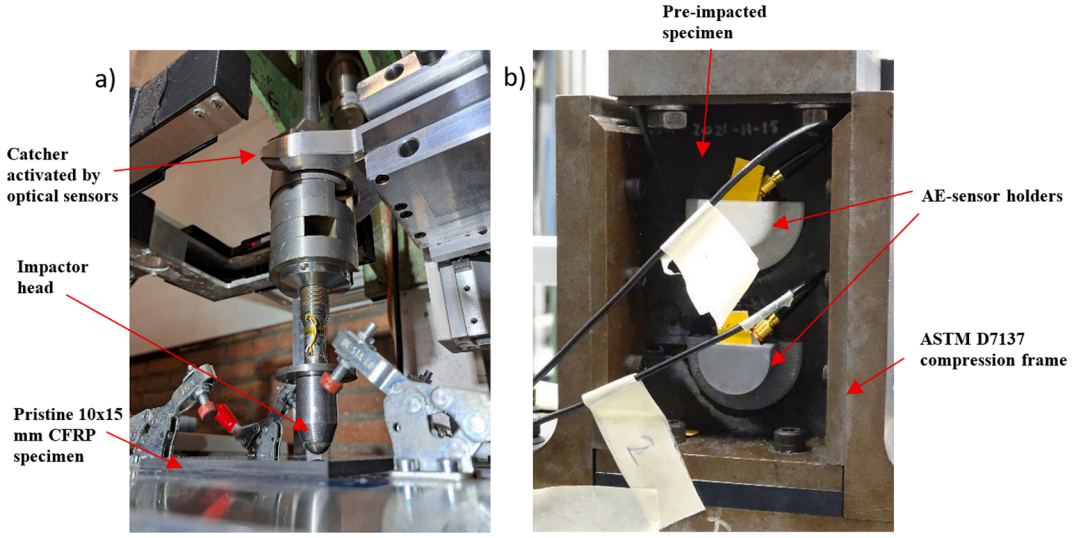

Fig. 2. (a) Impact test fixture; (b) CFAI fixture showing acoustic sensors and the respective holders.

Dolphicam 2 system, equipped with a scanning probe operating at 8 MHz. The through thickness attenuation system was selected to avoid the reflection effects that can arise from the top surface of the specimen in the dent region and to enable detection of delamination growth beneath the impact dent area. The echo pulse scan, on the other hand, was used to identify the delamination depths by determining the time of flight of reflected signals.

2.5. Acoustic emission acquisition

The AE activity was monitored by using two AE sensors placed on one side of the specimens (Fig. 2.b). The used AE sensor was the AE1045SVS900M, a broadband single-crystal piezoelectric transducer with operational frequency range of 100–900 kHz supplied by Vallen Systeme GmbH. To amplify the recorded signals, an external 34 dB pre-amplifier was used, and an acquisition threshold of 60 dB was set to reduce noise. The AE data was collected with a sampling frequency of 2 MHz using the AMSY-6 Vallen, 4-channel AE system. To improve the coupling between the AE sensor and the specimen's surface, ultrasound gel was used. The two sensors were kept in position using plastic sensor holders glued to the non-impacted surface of the specimen. The performance of the AE system was validated before each test by a standard pencil lead break procedure.

2.6. Acoustic emission noise reduction

A data analysis strategy was developed to deal with noise. In this case we refer to noise as the group of signals that are not related to damage

propagation. This acoustic activity can have several sources, such as friction between crack surfaces, contacts with the fixture and reflections.

1. The first level of noise reduction consisted in applying a relatively high amplitude threshold for the acquisition of transient waveforms (60 dB). This was decided to reduce the noise and to work with a smaller size of AE data. However, it must be considered that AE signals originating from matrix micro cracking and other low energy damage modes may be excluded by setting a threshold this high.
2. The second step was to only include signals happening at loads >80 % of the maximum amplitude in fatigue loading. This was decided assuming that damage within the load cycle is formed predominantly at higher compression loads.
3. The analysis of the waveforms recorded with this setting, revealed a low frequency (60 kHz) continuous-type signal which we associated with friction. Signals coming from damage are expected to be burst-type signals, rising and decaying in a very short time, while friction and noise are assumed to be a more 'continuous' type of signal. Considering this, a high pass filter allowing only frequencies >70 kHz was applied.
4. After this, to further improve the quality of the recorded AE signal, a four-level discrete wavelet packet filter was applied using Daubechies 32 wavelets, setting a hard threshold at 10 % of the maximum coefficient. Wavelets transforms allow to analyse the signals in the time and frequency domain [24]. Wavelet filters have proven to be capable to isolate bust type signals from background noise, hence they were selected for this specific application.
5. Once the AE signals were filtered, a 1-D localization was performed. Thanks to this procedure, it was possible to exclude from the analysis events that could not be localized in the area separating the two AE sensors, such as reflections. To effectively determine the arrival time of each hit, the energy ratio criterion was adopted [25].

3. Results and discussion

3.1. Impact test

The low velocity impact tests resulted in barely visible impact damages (BVID) characterized by impact dents of <0.3 mm depth. As can be seen from the three-dimensional reconstruction of impact damage, created with the Dolphicam 2 system (Fig. 3.a), the impact damage structure comprises multiple delaminations located in different interfaces. As reported by previous literature, delaminations tend to grow in every interface, bounded by the orientations of the upper and lower plies. Considering this, if the mismatch angle between consecutive plies is kept constant at 45 degrees through the laminate's layup, the delamination envelope will appear like a spiral composed of triangular shapes, all characterized by the same 45 degrees angle. This feature was documented in previous literature [15]. A central area with less attenuation can be observed in the through thickness transmission scan (Fig. 3.b), indicating that no delamination was formed during the impact in the area below the impact dent. The presence of this feature was discussed in the introduction and can be attributed to the out of plane compression originating in the contact between the impactor and the composite plate, which reduces the mode II strain energy release rate and acts as inhibitor to the delamination propagation. It is important to notice here that, while the non-delaminated region is clearly visible from a through thickness scan, it is hard to detect this feature using an echo pulse system. This because of the echo generated by the curved surface of the impact dent.

3.2. Fatigue after impact test

Five specimens were tested in fatigue after impact. Two specimens (SP-1, SP-2) were monitored using periodic through thickness scan inspections. Three specimens (SP-3, SP-4, SP-5) were monitored using periodic echo pulse scan inspections. The specimens were tested with different load levels to obtain both short and long fatigue lives. The maximum compression load level was defined as a fraction of average compressive strength after impact (CSAI) derived from previous static tests. A scheme of the performed tests can be found in Table 1. SP-3 was initially tested at a maximum compression stress of 65 % of CAI strength but produced no growth after 101,000 cycles, hence the load was increased to 75 % of CAI strength. At the new load level, the specimen failed after 94,000 cycles. SP-4 was initially tested at a maximum compression stress of 75 % of CAI strength but produced no growth after 179,400 cycles, hence the load was increased to 80 % of CAI strength. At

Table 1
Scheme of the performed fatigue test containing load level, applied inspection, fatigue life.

Name	Max comp. load [% CSAI]	Inspection procedure	Life [N cycles]
SP-1	65 %	T-T scan	180,000
SP-2	85 %	T-T scan	2,500
SP-3	65 %–75 %	E-P scan	195,000
SP-4	75 %–80 %	E-P scan	189,000
SP-5	80 %	E-P scan	5,600

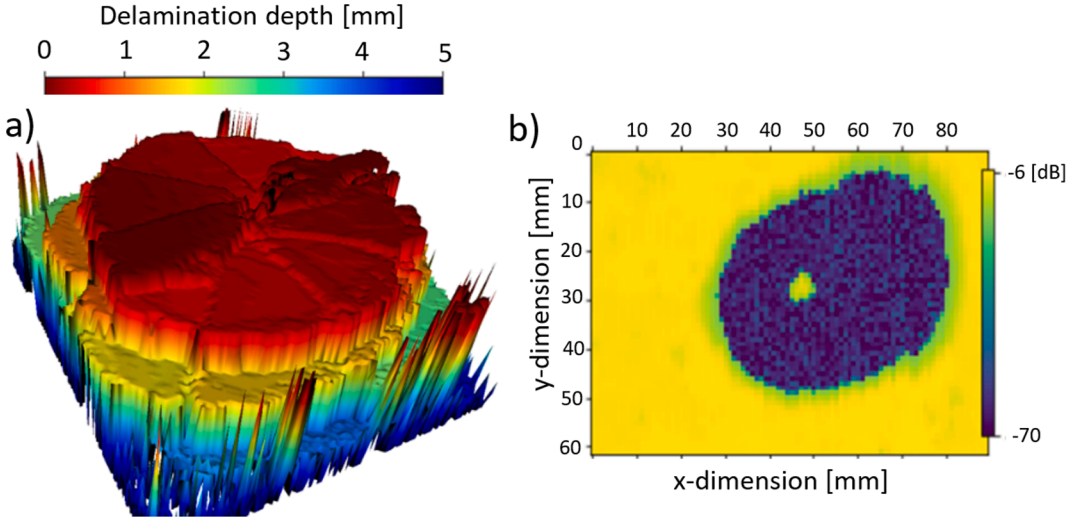

Fig. 3. Impact damage characterization using (a) echo pulse scan and (b) through thickness attenuation.

the new load level the specimen failed after 9,600 cycles.

In all specimens, final failure was characterized by unstable delamination propagation in multiple interfaces and fiber kinking. The fractured specimens appear very similar to previous static CAI tests previously conducted by the authors, showing a final fracture that runs in the centre of the specimen, perpendicular to the loading direction (Fig. 4).

3.3. Through transmission scan

In two of the tested specimens, we used through thickness attenuation scan to evaluate growth below the impact contact point. As explained in previous sections, there is an area below the impact point, where little or no delamination is present. Because of the impact dent reflection, it was difficult to evaluate this area using the echo-pulse system. For that reason we adopted through thickness transmission scan. The results clearly showed how the delamination propagation firstly happened in the central area, and only after that, a single delamination started growing towards the lateral edges (Fig. 5). These results seem to suggest that the phenomenon observed by Bull et al. in static tests [16], can occur also in fatigue. This phenomenon was observable only in the long-life fatigue specimen, in the short life, it was impossible to measure growth. In this case all the growth leading to failure happened in the interval between two inspections. Since we were able to observe the growth in the impact cone only once, we present this result of a proof of the fact that this phenomenon can indeed occur. It is still not clear if this growth happens systematically and what is the relationship with the geometrical features of the initial impact damage, such as the size of the non-delaminated cone and the shape of delaminations.

3.4. Echo-pulse scan

In the second batch of specimens, we used an echo pulse scan system to determine delaminations' depth with high accuracy. The monitoring revealed similar patterns of delamination growth regardless of the applied load level (Fig. 6). In the initial stages of fatigue, all the specimens displayed the growth of a single delamination situated close to the impacted face, propagating perpendicular to loading from impact center towards the lateral edges (Fig. 7). This short delamination grew within the projected delaminated area, hence during the phase that previous studies classified as a plateau phase in delamination growth. This growth was observable since it occurred close to the front face and was not shadowed. However, since impact damage consists of multiple delaminations located in almost every interface, we cannot exclude the possibility that faster growth of short delaminations occurred in the central depths during this phase, but was undetectable. This observation partially confirms the hypothesis formulated by Pascoe [12], suggesting that the apparent no-growth phase could be a consequence of the inability to measure shadowed growth using ultrasound inspection.

In the final stages of fatigue, delamination started growing outside of the projected delaminated area (Fig. 7, Fig. 8). At this stage, deep delaminations also grew in the transverse direction perpendicular to loading, but no growth was recorded in the loading direction throughout the test. The preferential growth in the perpendicular to loading direction is a pattern consistently found in the literature, except for the early work by Mitrovic et al. [11], where propagation parallel to the loading direction was observed. However, the test fixture used in that study was different from the standard static CAI test fixture and had a much more elongated shape in the loading direction without anti-buckling guides. This confirms that there is a high dependency of the results on the adopted test fixture.

Fig. 4. Failed specimen after the CFAI test.

Regarding the position in depth of the delamination propagation, previous studies with the same fixture reported the preferential growth of delamination close to the back face close to failure [8], while in our study, we consistently observed the growth of delamination situated in interfaces close to the front face, regardless of the applied load level. This demonstrates that even when the same fixture is used, there is a large variability in results due to different layups, material systems, and initial impact damage shape.

3.5. Acoustic emission

In addition to ultrasound monitoring, we analysed acoustic emission and performed damage mode separation. We collected and filtered the acoustic emission data as described in the methodology section. Then, we applied a fast Fourier transform to the transient signals using the Python NumPy library. Frequency features are known to be less affected by attenuation effects and can effectively discriminate between damage modes [20]. In a previous study, we conducted static tests on unidirectional layups at 90 degrees and 0 degrees to isolate and study waveforms originating from different damage modes [22]. The results clearly indicated that matrix cracking is characterized by lower frequency content compared to other damage modes, such as debonding and fiber fracture. Therefore, we selected the averaged peak frequency $\langle f_{peak} \rangle$, given by the equation below, as the discriminator parameter to separate damage modes.

$$f_{centroid} = \frac{\sum_{n=0}^{N-1} f(n)x(n)}{\sum_{n=0}^{N-1} x(n)} \tag{1}$$

$$\langle f_{peak} \rangle = \sqrt{f_{peak} * f_{centroid}} \tag{2}$$

where $x(n)$ represents the weighted frequency magnitude, of segment number n, and $f(n)$ represents the center frequency of that segment.

Fig. 9 presents the results of acoustic emissions, combined with ultrasound scans to investigate the different stages of fatigue life in short-life fatigue (SP-5) and long-life fatigue (SP-3). Interestingly, both short and long fatigue life exhibit an initial phase in which no growth is detected with C-scan, not even the growth of shorter delaminations. However, plenty of acoustic activity was measured during this phase, with a large part of it localized in the impact damage area and characterized by predominantly low frequency events. Due to the low frequency of the events and the fact that no growth of shorter delaminations was recorded during this initial phase, our hypothesis is that intralaminar matrix cracking was the main mechanism responsible for this acoustic activity. There is also the possibility that a growth of delamination in the shadowed area is responsible for this activity. Both hypotheses remain valid, since our previous investigation showed that we can't distinguish intra laminar matrix cracking from interlaminar matrix cracking using simple frequency parameters [22].

On the other hand, high frequency events, associated to fiber fractures, occurred predominantly close to the final failure. However, high frequency events were also observed in the early stages of fatigue life, in particular at the beginning of long-life fatigue test (SP 3). Our hypothesis is that fibers partially damaged during the impact test, fail during the very first load cycles. After these failures, a more stable phase is reached in which matrix damage is added predominantly, until a certain

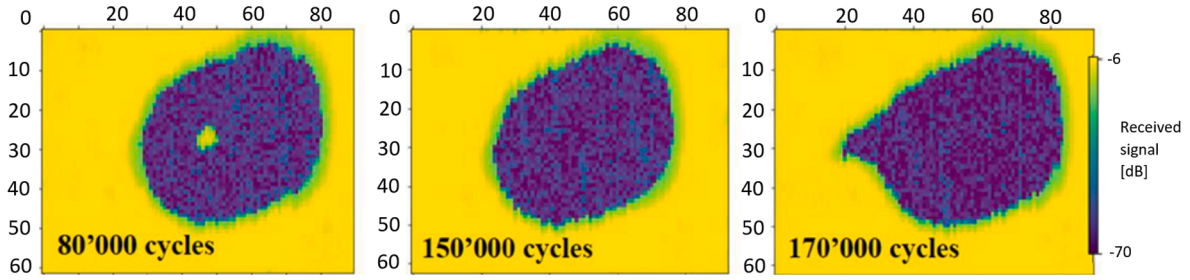

Fig. 5. SP-1 Delamination growth monitoring using through thickness transmission scan [27].

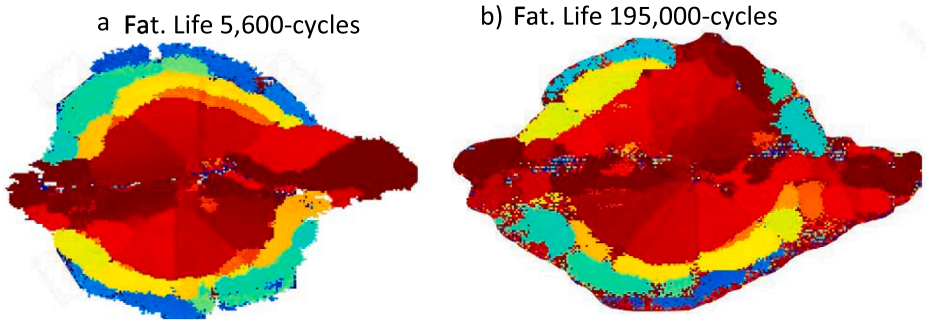

Fig. 6. C-scan of (a) short life (SP-5) and (b) long life (SP-4) specimens compared at >90 % of their respective fatigue lives.

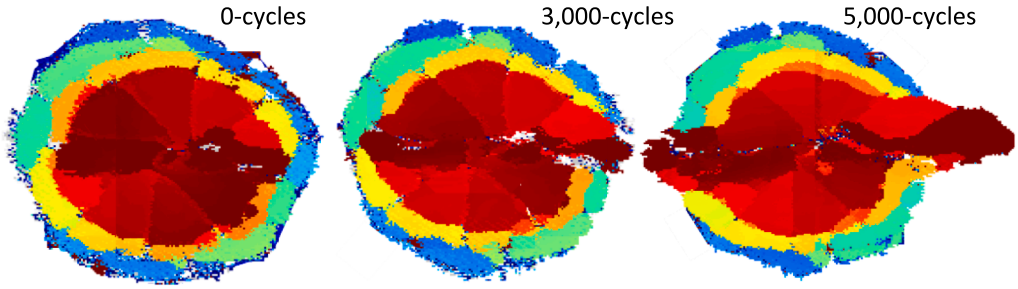

Fig. 7. SP-5 Delamination growth monitoring using through thickness transmission scan.

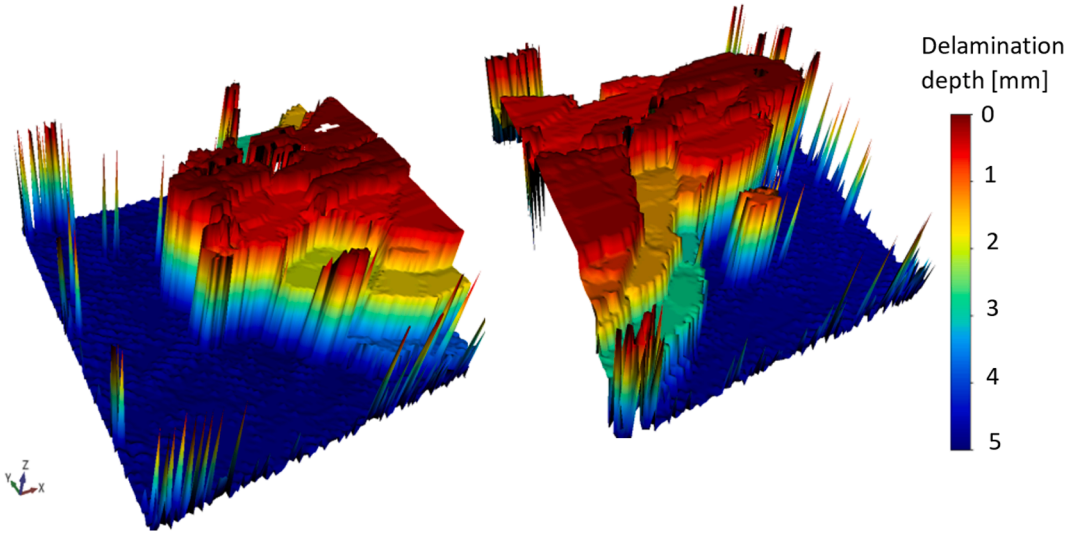

Fig. 8. 3D SP-5 Reconstruction of damage left and right sides propagated delamination.

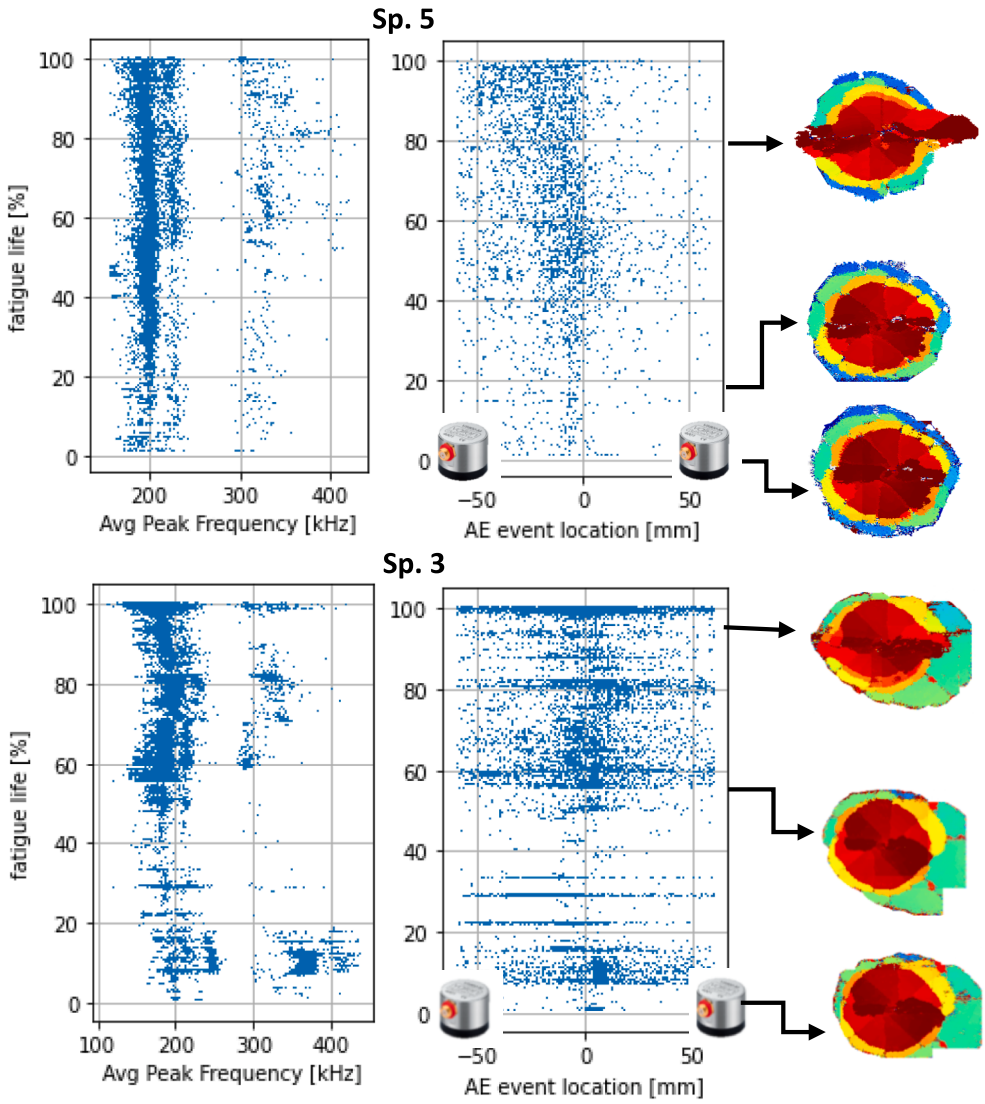

Fig. 9. Acoustic activity of short life specimen (top) and long life specimen (bot). Average frequency and localization result are plotted throughout the respective fatigue lives in comparison with c-scan inspections.

threshold of damage accumulation is reached allowing for a new fiber failure. From a more general perspective, acoustic activity associated to damage is not added at a constant rate, rather the opposite. We observed phases of high energy activity followed by phases of less acoustic activity. The phases of higher energy release seemed to be correlated in the long life fatigue test to the high frequency events.

4. Conclusions

An experimental campaign was conducted to investigate the phenomenon of plateau phase in fatigue after impact delamination growth. Two types of ultrasound scan (through transmission scan and echo pulse scan) were used to monitor delamination growth. Combining the two systems, an accurate reconstruction of delamination growth was provided, showing the same pattern of growth for both long and short fatigue lives. In combination with ultrasound monitoring, acoustic emissions were recorded and analysed. To be able to do that, a strategy to reduce the noise and the data size specific for CFAI testing was developed. Thanks to that it was possible to perform frequency analysis of acoustic signals throughout the entire fatigue tests. The outcome of this investigation was that, during the plateau phase of the projected impact delamination area growth, other damage accumulation mechanisms were active:

- By using through transmission ultrasonic inspection procedure, it was possible to observe the growth in the non-delaminated cone, a phenomenon previously observed only in static tests.
- By using an echo-pulse system it was possible to detect the preferential growth of shorter delaminations within the projected delamination impact area.
- By analyzing acoustic emissions, a low frequency activity localized in the impact damage area was recorded, even when no delamination growth was observed with the ultrasound systems. This activity could be either matrix cracking or growth of shadowed delaminations.

A first consideration to be made is that all three techniques applied in the present work, provided different information, and thus had to be combined to get a full picture of damage growth in fatigue. This shows that results obtained combining multiple NDI techniques are superior compared to those obtained relying uniquely on a single monitoring technique, as highlighted by previous research [26].

The conclusion of the present work is that the plateau phase in fatigue damage growth probably does not exist. It is possible that previous

authors observed a plateau phase due to limitations of the applied inspection techniques. Furthermore, the projected delamination area or width are insufficient to fully describe the damage growth. A suggestion for future experimental works is to combine information from multiple monitoring techniques and to adopt better damage descriptions to describe the process of fatigue growth in all its phases. More specifically the adopted damage growth characterization should include the growth in the undamaged cone and the growth of short delaminations inside the projected area. A next step for future research could be to determine whether propagation of intralaminar matrix cracks and shadowed delamination growth are also happening by employing computed tomography (CT) scan.

CRediT authorship contribution statement

Davide Biagini: Conceptualization, Data curation, Methodology, Writing - original draft, Writing - review & editing. **John-Alan Pascoe:** Conceptualization, Supervision, Methodology, Writing – review & editing. **René Alderliesten:** Conceptualization, Supervision, Methodology, Writing – review & editing.

Declaration of Competing Interest

The authors declare that they have no known competing financial interests or personal relationships that could have appeared to influence the work reported in this paper.

Data availability

Data will be made available on request.

Acknowledgements

We express our thanks to Dr. Rosemere De Araujo Alves Lima (TU Delft Faculty of Aerospace Engineering, Aerospace Structures & Materials) for stimulating discussions and feedback regarding acoustic emission analysis and localization.

References

[1] Abrate S. Impact on laminated composite materials. Appl Mech Rev 1991;44(4):155–90. https://doi.org/10.1115/1.3119500.
[2] Hull D, Shi YB. Damage mechanism characterization in composite damage tolerance investigations. Compos Struct 1993;23(2):99–120. https://doi.org/10.1016/0263-8223(93)90015-I.
[3] Chen AS, Almond DP, Harris B. Impact damage growth in composites under fatigue conditions monitored by acoustography. Int J Fatigue 2002;24(2–4):257–61. https://doi.org/10.1016/S0142-1123(01)00080-9.
[4] Nettles AT, Scharber L. The influence of GI and GII on the compression after impact strength of carbon fiber/epoxy laminates. J Compos Mater 2018;52(8):991–1003. https://doi.org/10.1177/0021998317719567.
[5] Melin LG, Schön J, Nyman T. Fatigue testing and buckling characteristics of impacted composite specimens. Int J Fatigue 2002;24(2–4):263–72. https://doi.org/10.1016/S0142-1123(01)00081-0.
[6] Melin LG, Schön J. Buckling behaviour and delamination growth in impacted composite specimens under fatigue load: an experimental study. Compos Sci Technol 2001;61(13):1841–52. https://doi.org/10.1016/S0266-3538(01)00085-9.
[7] Davies G, Irving P. Impact, post-impact strength, and post-impact fatigue behavior of polymer composites. Elsevier Ltd; 2020. doi: 10.1016/b978-0-08-102679-3.00011-3.
[8] Tuo H, Wu T, Lu Z, Ma X. Evaluation of damage evolution of impacted composite laminates under fatigue loadings by infrared thermography and ultrasonic methods. Polym Test 2021;93. https://doi.org/10.1016/j.polymertesting.2020.106869.
[9] Ogasawara T, Sugimoto S, Katoh H, Ishikawa T. Fatigue behavior and lifetime distribution of impact-damaged carbon fiber/toughened epoxy composites under compressive loading. Adv Compos Mater 2013;22(2):65–78. https://doi.org/10.1080/09243046.2013.768324.
[10] Clark G, Van Blaricum TJ. Load spectrum modification effects on fatigue of impact-damaged carbon fibre composite coupons. Composites 1987;18(3):243–51. https://doi.org/10.1016/0010-4361(87)90414-9.
[11] Mitrovic M, Hahn HT, Carman GP, Shyprykevich P. Effect of loading parameters on the fatigue behavior of impact damaged composite laminates. Compos Sci Technol 1999;59(14):2059–78. https://doi.org/10.1016/s0266-3538(99)00061-5.
[12] Pascoe JA. Slow-growth damage tolerance for fatigue after impact in FRP composites: Why current research won't get us there. Theor Appl Fract Mech 2021;116. https://doi.org/10.1016/j.tafmec.2021.103127.
[13] Federal Aviation Administration. Advisory circular AC20-107B composite aircraft structure; 2010.URL:https://www.faa.gov/documentLibrary/media/Advisory_Circular/AC_20-107B_with_change_1.pdf.
[14] European Aviation Safety Agency. Annex II - AMC 20-29 to ED Decision 2010/003/R - EASA.
[15] Ellison A, Kim H. Shadowed delamination area estimation in ultrasonic C-scans of impacted composites validated by X-ray CT. J Compos Mater 2020;54(4):549–61. https://doi.org/10.1177/0021998319865311.
[16] Bull DJ, Spearing SM, Sinclair I. Observations of damage development from compression-after-impact experiments using ex situ micro-focus computed tomography. Compos Sci Technol 2014;97:106–14. https://doi.org/10.1016/j.compscitech.2014.04.008.
[17] Saeedifar M, Zarouchas D. Damage characterization of laminated composites using acoustic emission: a review. In: Composites Part B: Engineering. Vol. 195. Elsevier Ltd; Aug. 15, 2020. doi: 10.1016/j.compositesb.2020.108039.
[18] Muir C et al. Damage mechanism identification in composites via machine learning and acoustic emission. npj Comput Mater 2021;7(1). Nature Research. doi: 10.1038/s41524-021-00565-x.
[19] Saeedifar M, Najafabadi MA, Zarouchas D, Toudeshky HH, Jalalvand M. Clustering of interlaminar and intralaminar damages in laminated composites under indentation loading using Acoustic Emission. Compos B Eng 2018;144:206–19. https://doi.org/10.1016/j.compositesb.2018.02.028.
[20] Sause MGR, Horn S. Simulation of acoustic emission in planar carbon fiber reinforced plastic specimens. J Nondestr Eval 2010;29(2):123–42. https://doi.org/10.1007/s10921-010-0071-7.
[21] Arumugam V, Adhithya Plato Sidharth A, Santulli C. Characterization of failure modes in compression-after impact of glass–epoxy composite laminates using acoustic emission monitoring. J Braz Soc Mech Sci Eng 2015;37(5):1445–55. doi: 10.1007/s40430-014-0263-7.
[22] Biagini D, Pascoe J-A, Alderliesten R. Investigation of compression after impact failure in carbon fiber reinforced polymers using acoustic emission. J Compos Mater 2023:002199832311638. doi: 10.1177/00219983231163853.
[23] Saeedifar M, Saleh MN, El-Dessouky HM, Teixeira De Freitas S, Zarouchas D. Damage assessment of NCF, 2D and 3D woven composites under compression after multiple-impact using acoustic emission. Compos Part A: Appl Sci Manuf 2020;132. https://doi.org/10.1016/j.compositesa.2020.105833.
[24] Graps A. An introduction to wavelets. IEEE Comput Sci Eng 1995;2(2):50–61. https://doi.org/10.1109/99.388960.
[25] Han L, Wong J, Bancroft JC. Time picking and random noise reduction on microseismic data; 2009.
[26] Broer A, Galanopoulos G, Benedictus R, Loutas T, Zarouchas D. Fusion-based damage diagnostics for stiffened composite panels. Struct Health Monit 2022;21(2):613–39. https://doi.org/10.1177/14759217211007127.
[27] Biagini D, Pascoe JA, Alderliesten RC. Experimental investigation of fatigue after impact damage growth in CFRP. Proc Struct Integr 2022;42:343–50. https://doi.org/10.1016/j.prostr.2022.12.042.